7194–7205 *Nucleic Acids Research, 2009, Vol. 37, No. 21* *Published online 22 September 2009*
doi:10.1093/nar/gkp767

A trimeric DNA polymerase complex increases the native replication processivity

Andrey L. Mikheikin[1], Hsiang-Kai Lin[1], Preeti Mehta[2], Linda Jen-Jacobson[2] and Michael A. Trakselis[1,*]

[1]Department of Chemistry, [2]Department of Biological Sciences, University of Pittsburgh, Pittsburgh, PA 15260, USA

Received May 26, 2009; Revised August 31, 2009; Accepted September 1, 2009

ABSTRACT

DNA polymerases are essential enzymes in all domains of life for both DNA replication and repair. The primary DNA replication polymerase from *Sulfolobus solfataricus* (*Sso*Dpo1) has been shown previously to provide the necessary polymerization speed and exonuclease activity to replicate the genome accurately. We find that this polymerase is able to physically associate with itself to form a trimer and that this complex is stabilized in the presence of DNA. Analytical gel filtration and electrophoretic mobility shift assays establish that initially a single DNA polymerase binds to DNA followed by the cooperative binding of two additional molecules of the polymerase at higher concentrations of the enzyme. Protein chemical crosslinking experiments show that these are specific polymerase–polymerase interactions and not just separate binding events along DNA. Isothermal titration calorimetry and fluorescence anisotropy experiments corroborate these findings and show a stoichiometry where three polymerases are bound to a single DNA substrate. The trimeric polymerase complex significantly increases both the DNA synthesis rate and the processivity of *Sso*Dpo1. Taken together, these results suggest the presence of a trimeric DNA polymerase complex that is able to synthesize long DNA strands more efficiently than the monomeric form.

INTRODUCTION

DNA polymerases are highly conserved enzymes found in all domains of life, and depending on the type, are primarily responsible for DNA replication or repair activities. Many of the structural and mechanistic features of these polymerases are shared across a broad range of organisms, but slight differences have been identified with regards to substrate specificity, template sensing, as well as coordinating polymerase and exonuclease activities (1–4). The genome of *Sulfolobus solfataricus (Sso)* contains DNA polymerase members from both the DNA replication B-family as well as a lesion bypass polymerase from the Y-family (5,6). The B-family DNA polymerase (*Sso*Dpo1) has been shown to have the necessary enzymatic and kinetic properties to be the replicative polymerase in *Sulfolobus* (7–12). A crystal structure of *Sso*Dpo1 has been solved showing a typical right-handed conformation of the polymerase with an extended fingers domain hypothesized to be involved in either conformational changes involved in catalysis or protein–protein interactions (13). Under normal DNA replication conditions, *Sso*Dpo1 is thought to interact with the heterotrimeric *Sso*PCNA complex (14,15) to maintain a high degree of processivity (16) and possibly with the Y-family DNA polymerase, *Sso*Dpo4, to bypass DNA lesions (17). This common tool belt model of protein interactions has been suggested to be important in increasing the local concentrations of proteins, especially DNA polymerases, at the replication fork to maintain the speed and accuracy needed for successful DNA replication (18). This is even more evident with the many other known stable interactions with proliferating cell nuclear antigen (PCNA) within the cell (19).

Polymerase–polymerase interactions either directly or indirectly are also necessary for coordinated DNA replication on both the leading and lagging strands. Direct evidence of a polymerase interaction was detected by protein crosslinking in bacteriophage T4 (20). In addition, a dominant negative form of the T4 polymerase was shown to shut down DNA replication in a coordinated replisome, suggesting the utilization of a dynamic polymerase-switching mechanism during DNA replication (21). In *E. coli*, polymerase coupling is mediated through

*To whom correspondence should be addressed. Tel: +1 412 624 1204; Fax: +1 412 624 8611; Email: mtraksel@pitt.edu

the tau subunit (22). In fact, a trimeric polymerase complex in which three copies of tau are incorporated into the clamp loader complex has been shown to be fully active on both the leading and lagging strands and may be an important factor in maintaining efficient Okazaki fragment processing (23). In higher eukaryotes, it is currently unknown how the replication polymerases, ε and δ, are coordinated on the leading and lagging strands, respectively (24), but they are thought to have specific yet unknown plastic interactions with accessory proteins and themselves to maintain the replication fork (25).

Because of a large distance between the polymerase and exonuclease active sites in most DNA polymerases, it has been suggested that there may be multiple polymerase-bound conformations. Co-crystal structures of *E. coli* Klenow polymerase and the homologous version in *Thermus aquaticus* bound to primer/template DNA identify separate polymerization and editing modes of binding (26–28). A recent report shows that Klenow can bind to primer/template DNA as a monomer or dimer, but the dimer form is more prevalent in the polymerization mode (29). Effects of polymerase multimerization either alone or in concert with accessory factors may have important implications in maintaining high processivity as well as coordinated DNA synthesis between the leading and lagging strands.

In this report, we have used a variety of biochemical techniques to investigate the stoichiometry of *Sso*Dpo1 on DNA and show that the oligomeric state influences the mechanism of polymerization. We have determined that *Sso*Dpo1 binds to a DNA primer/template initially as a monomer and cooperatively forms a trimeric polymerase complex with increasing concentrations. This trimeric complex can increase both polymerase kinetic activity and processivity. The organization of this multimeric polymerase is discussed with regard to binding conformation and effect on polymerization kinetics and has important implications for DNA replication mechanisms.

MATERIALS AND METHODS

Materials and their sources

Oligonucleotide substrates were purchased from Integrated DNA Technologies (IDT) (Coralville, IA) (For substrates and sequences see Supplementary Data). Gel purification of the DNA strands was performed as previously described (30). Primer/template and duplex substrates were prepared by mixing each strand in 1:1 ratio in a buffer containing 20 mM Tris (pH 7.5) and 200 mM NaCl. The annealed complex was heated at 95°C for 2 min and allowed to cool down slowly for at least 2 h in the heat block. M13mp18 was purchased from USB Corporation (Cleveland, OH). All radiochemicals were purchased from MP Biochemicals (Santa Ana, CA). Commercial enzymes were from NEB (Ipswich, MA). All other chemicals were analytical grade or better.

*Sso*Dpo1 was amplified from genomic *S. solfataricus* P2 (ATCC, Manassas, VA.) using *Pfx*50 polymerase (Invitrogen, Carlsbad, CA). Initial ligation of the PCR product into pGMET (Promega, Madison, WI) was performed using standard T-cloning. Standard QuikChange protocol (Stratagene, La Jolla, CA) was used to create an exonuclease mutant of SsoDpo1 (D231A/D318A). Specific restriction sites *AseI* and *XhoI* contained in the primers were used to clone *Sso*Dpo1 into pET30a digested with *NdeI* and *XhoI* (Novagen) to include a C terminal His tag. The *Sso*Dpo1 exonuclease mutant (D231A/D318A) was used hereafter in all studies described in this manuscript. DNA sequences were verified by the Genomics and Proteomics Core Laboratories at the University of Pittsburgh.

*Sso*Dpo1 expression and purification

pET30a-*Sso*Dpo1 exo$^-$ was transformed into BL21(DE3) Rosetta 2 (Stratagene) and grown at 37°C. Cells were induced with 0.5 mM IPTG at OD_{600} between 0.5 and 0.6. The cells were lysed by sonication and heat treated at 70°C for 30 min followed by centrifugation. The lysate supernatant was purified further by Ni-NTA agarose, heparin and SP sepharose columns (GE Healthscience). Final cleanup and size selection was performed using a Superdex 200 26/60 gel filtration column. The extinction coefficient for *Sso*Dpo1 was calculated to be 118 282 $M^{-1}\,cm^{-1}$ (31).

Analytical gel filtration

Superdex 200 10/30 column (GE Healthscience) was used at a flow rate of 0.2 ml min^{-1} in Buffer A [20 mM HEPES−NaOH (pH 7), 240 mM NaCl, 5% Glycerol, 10 mM $Mg(OAc)_2$, 0.2 mM DTT] and protein elution was monitored at 280 nm. Binding and kinetic experiments were performed using identical buffer conditions (Buffer A) unless indicated otherwise. The molecular ruler standards Thyroglobin (165 kDa, Sigma), Conalbumin (75 kDa, GE Healthscience), Albumin (43 kDa, Sigma), Myoglobin (17.6 kDa, Sigma) and Vitamin B12 (1.4 kDa, Sigma) were run to create a standard log curve fit by linear least squares. One hundred microliters *Sso*Dpo1(100 μM) in the absence or presence of DNA substrates at concentrations of 20 μM was injected with the internal standard, vitamin B12, added for monitoring any elution shift. The molecular weight of the eluting species was calculated from the standard log plot.

Electrophoretic mobility shift assay

Electrophoretic mobility shift assays (EMSAs) were performed in a 10 μl reaction volume containing Buffer A with 4 nM DNA probe labeled at the 5′-end using a standard polynucleotide kinase reaction and ^{32}P-γ-ATP, and the indicated amount of *Sso*Dpo1. Binding reactions were allowed to equilibrate for 10 min followed by directly loading onto a gradient 4–15% polyacrylamide/TBE ReadyGel (BioRad, Hercules, CA). Gels were run for 1 h at 13 volts cm^{-1} followed by drying and imaging using a Storm phosphorimager (GE Healthscience). Quantification of the fraction of band shift was performed using the ImageQuant software (v5.0).

Data were fit using non-linear least squares analysis using Kaleidagraph (Synergy, Reading, PA) to an equivalent multiple site binding model defined by

$$y = \frac{f_{\max} \times [P]^n}{K_d^n + [P]^n} \quad \mathbf{1}$$

where $f_{\max}$ is the maximum fraction shifted, P is the *Sso*Dpo1 concentration, K_d is the dissociation constant and n is the Hill coefficient which defines cooperativity.

Fluorescence anisotropy

Fluorescence anisotropy measurements were performed in Buffer A. A fluorescently labeled DNA hairpin 5′-Cy5-TT TTTTTTTTTTTTCGAATGGCGCTTTGCCTGGTT TTTACCAGGCAAAGCGCCATTCG that was HPLC purified (IDT) was used in all anisotropy experiments. Before measurements, the hairpin was heated to 95°C and then allowed to anneal slowly to room temperature over at least 1 h. Measurements were performed on FluoroMax-3 spectrofluorimeter (HORIBA Jobin Yvon). Fluorescence was excited at 645 nm, and the emission was monitored at 675 nm during 1-s integration times and represents an average of 10 consecutive readings. The absolute fluorescence intensity at 675 nm did not change with addition of a high concentration of *Sso*Dpo1 ruling out the possibility that *Sso*Dpo1 binds specifically to the Cy5 fluorophore. The fluorescence anisotropy, r, was calculated using the equation:

$$r = \frac{I_{VV} - GI_{VH}}{I_{VV} + 2I_{VH}} \quad \mathbf{2}$$

where I is the polarized fluorescence intensity with subscripts V and H identifying either vertical or horizontal polarized light, respectively. The G-factor is a correction for the difference in sensitivities of detection for horizontal and vertically polarized light, and was measured immediately before each experiment and is defined by

$$G = \frac{I_{HV}}{I_{HH}} \quad \mathbf{3}$$

The observed anisotropy is the sum of all the anisotropy values for each species present. In this case, only the DNA was labeled so there is no contribution from free protein. Only species containing DNA, either alone or *Sso*Dpo1-bound complexes contribute to the anisotropy, defined as

$$r = \sum_i f_i r_i \quad \mathbf{4}$$

where f_i is the fraction of an individual species and r_i is the associated anisotropy values. Contributions to anisotropy are therefore equal to

$$r = r_D[D] + r_{DP}[DP] + r_{DP_3}[DP_3] \quad \mathbf{5}$$

where r_D, r_{DP}, r_{DP3} are the anisotropy values for the DNA alone, singly bound *Sso*Dpo1 and trimeric *Sso*Dpo1-bound complexes, respectively.

Isothermal titration calorimetry

Isothermal titration calorimetry (ITC) was performed using VP-ITC (MicroCal Inc., Northampton, MA) at 303°K for *Sso*Dpo1 binding to DNA (32). Prior to the experiment, *Sso*Dpo1 and DNA were dialyzed in Buffer A. The concentrations of the dialyzed protein and DNA were determined prior to the titration. Typical titrations consisted of 30 injections of 2–5 µl of DNA solution (500 µM) into the overfilled (~1.4 ml) sample cell containing *Sso*Dpo1 (20 µM). To obtain the effective heat of binding, the observed heats of reaction were corrected for the heat of dilution of the DNA by subtracting the baseline heats obtained after saturation. All data were fit using Origin 7.0 (MicroCal) to the following equation (33)

$$Q = \left(\frac{n[P]t\Delta HV_0}{2}\right)\left\{1 + \frac{[D]_t}{n[P]_t} + \frac{1}{nK_a[P]_t} - \left[\left(1 + \frac{[D]_t}{n[P]_t} + \frac{1}{nK_a[P]_t}\right)^2 - \frac{4[D]_t}{n[P]_t}\right]^{1/2}\right\} \quad \mathbf{6}$$

where V_0 is the volume of the cell, ΔH is the enthalpy of binding per mole of ligand, $[P]_t$ is the total [*Sso*Dpo1] including both bound and free fractions, K_a is the binding constant, $[D]_t$ is the total DNA concentration and n is the stoichiometry of the reaction.

Crosslinking studies

We performed all crosslinking studies in buffer A and over a range of [NaCl]. Sulfo-EGS [ethylene glycol bis(sulfosuccinimidylsuccinate)] (Pierce, Rockford, IL) was used as the crosslinker targeting free amino groups. 10 µM of *Sso*Dpo1 was incubated with primer/template DNA (similar to ITC conditions) for 1 min at various temperatures, then crosslinker was added to a final concentration of 0.5 mM and the reaction mixture was incubated for 30 min at variant temperatures. The reaction was stopped by addition of 1 M Tris–HCl (pH 7.5) to a final concentration of 50 mM and then incubating at room temperature for 15 min. Products of crosslinking reaction were analyzed using a 6% SDS–PAGE gel and stained with Coomassie dye.

Polymerase kinetics

The polymerase assay monitored the incorporation of nucleotides on primer/template 5′ [γ-^{32}P]-labeled DNA substrates. Individual primer strands were first labeled with [γ-^{32}P ATP] using a standard PNK reaction and then annealed to M13mp18 or 31-mer ssDNA. The reaction was started by mixing labeled DNA substrates (4 nM), dNTPs (0.05 mM), reaction buffer and *Sso*Dpo1 at various concentrations and incubating at 37 or 60°C for various times. For single-turnover processivity experiments, *Sso*Dpo1 was preassembled on ptDNA and the reaction was initiated with dNTPs and a 5000-fold excess of ssDNA as a polymerase trap at 37 or 60°C. One volume of stop solution (100 mM EDTA, 0.1% SDS, 80% Formamide, 0.1% Bromophenol Blue) was

added to terminate the reaction. Aliquots were run on either a denaturing (14% Acrylamide/8M Urea/1X TBE) or alkaline agarose (0.8% agarose, 1N NaOH, 0.5 M EDTA) gel, dried and phosphorimaged. Quantification of the band intensities and lengths was performed using ImageQuant software (v5.0). The calculated rate of DNA synthesis (bp/min or fraction of full length product) as a function of *Sso*Dpo1 concentration was initially fit to a standard Michaelis–Menten equation, but a fit that included a positive cooperativity parameter (n) for allosteric enzymes according to the following equation,

$$v = \frac{V_{\max} \times [P]^n}{K_D^{'n} + [P]^n} \quad (7)$$

gave a much better fit where $K_D^{'}$ is the apparent catalytic dissociation constant for *Sso*Dpo1 (P) and $V_{\max}$ is maximal rate of synthesis. The off-rate of the polymerase for each oligomeric state can be calculated by dividing the rate of DNA synthesis (bp/min) by the average processivity (bp) to give $\min^{-1}$.

RESULTS

Analysis of *Sso*Dpo1–DNA substrate complex formation by analytical gel filtration

During the purification as detected by both preparatory and analytical gel filtration, *Sso*Dpo1 exists as a monomer (101 kDa) and eluted alone at 13.5 ml (Figure 1). Addition of DNA was found to shift the equilibrium of binding to a higher molecular weight species consistent with the formation of a higher-order complex. Although lower concentrations of NaCl (100 mM) gave a larger proportion of the higher-order complex (data not shown), we used 240 mM NaCl contained in buffer A in further binding and kinetic assays to reduce any potential contributions of nonspecific aggregation events.

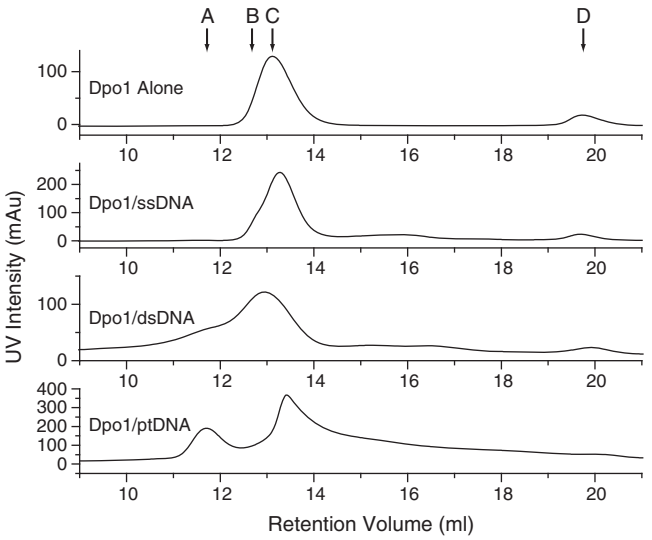

Figure 1. Gel filtration profile of a constant initial concentration of *Sso*Dpo1 (100 μM) and various DNA substrates (20 μM). Single strand (ssDNA) (31-mer), blunt duplex (dsDNA) (50/50-mer) and primer/template (p/tDNA) (21/31-mer) DNA are shown. Peaks identified as A, B and C represent trimer:DNA, monomer:DNA and monomer forms of *Sso*Dpo1, respectively according to fit of a standard molecular weight ruler. A constant concentration of vitamin B12 was used as an internal standard in all the experiments to account for drift in the elution profile (peak D).

To determine relative binding affinities for different DNA substrates, an identical initial loading concentration (100 μM) of *Sso*Dpo1 was incubated with separate DNA substrates and then analyzed by analytical gel filtration. The most obvious change in these elution profiles is from the complexation of *Sso*Dpo1 and p/tDNA (21/31) (Figure 1). This shifted peak (*bottom panel*) eluted at a position consistent with a trimeric *Sso*Dpo1 complex bound to DNA (as determined from the standard log curve with molecular weight markers). Complexes with single strand and with blunt duplex DNA were also compared under the same conditions. In both cases, a protein–DNA complex eluted in the position (unresolved from free monomeric protein) predicted for a monomeric *Sso*Dpo1–DNA complex. Blunt duplex DNA was able to stimulate the formation of a trimeric complex, significantly more than with ssDNA but less than p/tDNA.

It is possible that higher-order complexes exist on the single and double strand substrates at the high initial concentrations prior to injection, but because of dilution during the course of gel filtration chromatography, the equilibrium is driven to the lower-order monomeric *Sso*Dpo1—DNA species. The composition of the peaks C and B (Figure 1) consisting of monomer and monomer bound to DNA would therefore dominate the equilibrium after elution from the column for the single and dsDNA substrates.

EMSA of *Sso*Dpo1/DNA complexes

EMSAs were utilized to analyze the binding of *Sso*Dpo1 to 5′ [γ-^{32}P]-labeled ssDNA, dsDNA and primer/template (p/tDNA) substrates (Figure 2). *Sso*Dpo1 can bind to all substrates, since in all cases, a shift in the apparent molecular weight is observed. For *Sso*Dpo1 binding to ssDNA and dsDNA, only two bands are clearly observed on the gels (Figure 2A): lower band corresponds to unbound DNA (at [*Sso*Dpo1] < 150 nM) and upper one (at [*Sso*Dpo1] > 1500 nM) corresponds to *Sso*Dpo1–DNA complex. There is some evidence, just above a background level, of an intermediate band from 150 to 1500 nM *Sso*Dpo1 with the dsDNA template (Figure 2B) consistent with either a monomer or dimer of *Sso*Dpo1 bound to DNA. This monomeric or dimeric polymerase DNA complex was not reproducible due to its low abundance with some DNA substrates. Fitting these data to a model that analyzes the percent of DNA shifted, regardless of the complex state (Equation 1), identifies a cooperativity of binding leading to a stoichiometry of *Sso*Dpo1–DNA complex as 3:1 (Supplementary Figures S1A and B). Similar global binding affinities and stoichiometries are calculated for ss- and dsDNA templates (Table 1). These results cannot specifically rule out preferential binding of a preformed trimeric *Sso*Dpo1 complex to either substrate due to the low abundance of an intermediate

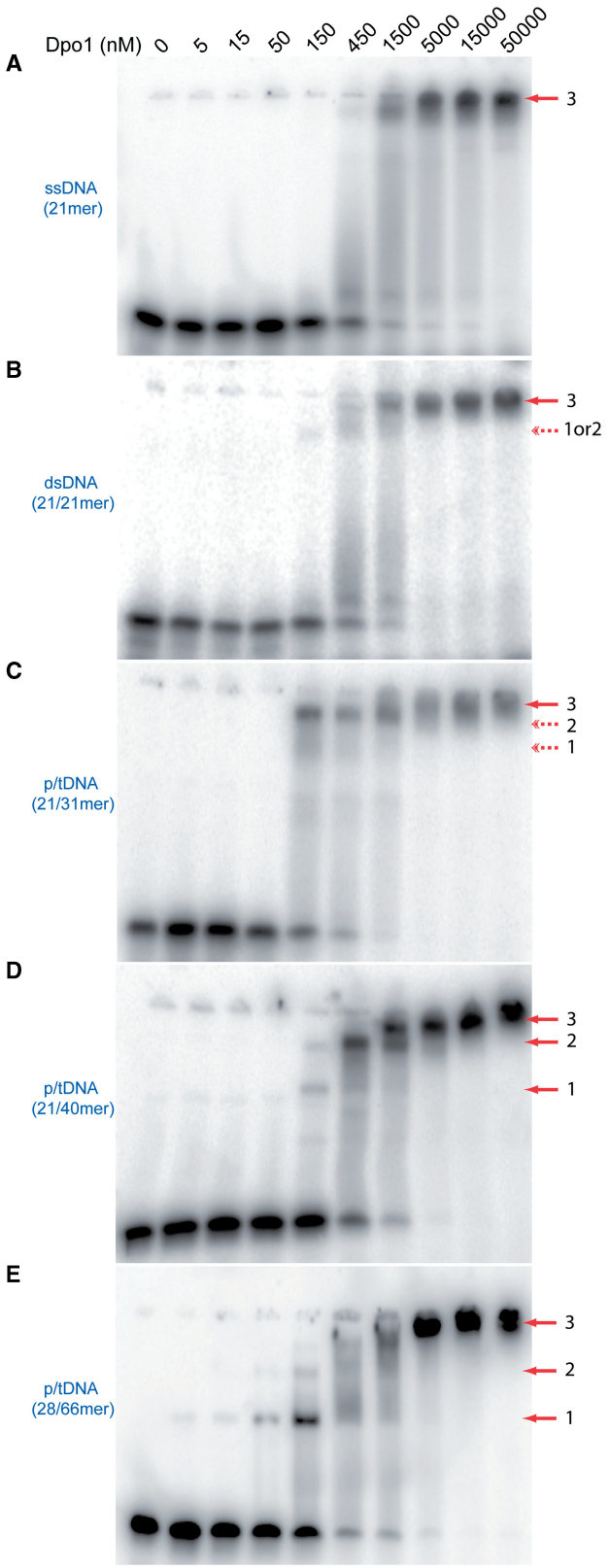

Figure 2. EMSA of the interaction of *Sso*Dpo1 with a variety of different DNA substrates labeled at the 5′-end with ^{32}P; (**A**) single strand (21-mer), (**B**) duplex DNA (21/21-mer), (**C**) short primer/template DNA (21/31-mer), (**D**) medium primer/template (21/40-mer) and (**E**) long primer/template DNA (28/66). The concentration of *Sso*Dpo1 was increased as shown above the gels identically for all experiments. The shift to the top of the gel identifies the trimeric polymerase complex highlighted by an *arrow* labeled with 3. The other *arrows* labeled 1 and 2 represent a monomeric and dimeric DNA complex, respectively. *Dashed arrows* represent extremely weak and faint complexes, while *solid arrows* are highly reproducible complexes. Fits of the fraction of DNA shifted are shown in Figure S2.

Table 1. Dissociation constants (K_T) and stoichiometries (n) of *Sso*Dpo1 binding to different DNA substrates determined by EMSAs

DNA substrate	K_T^a (nM)	Stoichiometry (n)
ssDNA(21-mer)	0.42 ± 0.02	2.8 ± 0.4
dsDNA (21/21-mer)	0.33 ± 0.02	2.7 ± 0.3
Short p/tDNA (21/31-mer)	0.27 ± 0.01	2.8 ± 0.1
Medium p/tDNA (21/40-mer)	0.23 ± 0.01	3.1 ± 0.2
Long p/tDNA (28/66-mer)	0.10 ± 0.01	3.0 ± 0.3

[a]The dissociation constant (K_T) represents the overall binding affinity of the total complex of *Sso*Dpo1 to DNA. In this analysis, it includes parameters from monomeric, dimeric and trimeric *Sso*Dpo1 binding to DNA.

band which could indicate either progression of *Sso*Dpo1 binding cooperatively or dimeric *Sso*Dpo1 binding directly to DNA.

In contrast, four bands are observed on the gels for the complex of *Sso*Dpo1 with p/tDNA substrates with increasing size (Figures 2C, D and E). These additional protein DNA complexes, barely visible with the dsDNA substrate above, are more pronounced with p/tDNA and appear at lower protein concentrations. These additional bands labeled 1 and 2 are more clearly seen in the case of p/tDNA with a longer single-stranded tail (Figure 2D and E). Bands 1 and 2 suggest the formation of another type of *Sso*Dpo1–DNA complex with an apparent lower molecular mass than the fully shifted protein DNA complex seen in Figure 2A and B. The stoichiometry of *Sso*Dpo1 binding to DNA was determined by performing an EMSA at high concentrations of DNA (7.5 μM) and stained with either ethidium bromide or coomassie blue (data not shown) and was found to be 3.5 ± 0.7 for *Sso*Dpo1:DNA.

Higher mobility of this type of complex in gel compared to the upper band 3 indicates a lower stoichiometry of this type of complex: either monomeric or dimeric (1 : 1 or 2 : 1 *Sso*Dpo1:DNA ratio, respectively). At [*Sso*Dpo1] > 150 nM, band 1 and eventually band 2 disappear and *Sso*Dpo1−DNA complex has mobility similar to the trimeric complex observed for ss- and dsDNA (see above). Fitting the percentage of DNA (fraction of total DNA) shifted above the free DNA position revealed a 3:1 *Sso*Dpo1:DNA stoichiometry (see Supplementary Figure 1C, D and E) (Table 1). Since band 1 appears at a lower [*Sso*Dpo1] concentration than in either the ssDNA or dsDNA EMSA, the monomeric *Sso*Dpo1 has a higher initial affinity (~3-fold) for p/tDNA compared to ss- and dsDNA and promotes the cooperative formation of a trimeric *Sso*Dpo1/DNA complex that proceeds first through a dimeric *Sso*Dpo1/DNA complex. At high concentrations of *Sso*Dpo1 for either the 21/40-mer or 28/66-mers substrate (Figure 2D and E), there may be a

percentage of complex that is above the molecular weight for the trimer. The resolution between trimer and higher complex states in these cases is small and difficult to differentiate. Binding of additional polymerase molecules (>3) to these longer templates at either the single strand or double strand ends may be responsible for these complexes.

To determine if this complex is binding along the length of these longer primer-template substrates or specifically at the primer-template junction, we used nuclease footprinting to map protected sites with increasing concentrations of *Sso*Dpo1 corresponding to monomer and trimer formation (Supplementary Figure S2). A reproducible footprint is observed at roughly 9–10 bases on either side of the primer-template junction for both monomer and trimer. A shift in the hypersensitivity of DNA cleavage by S1 nuclease upon binding of *Sso*Dpo1 identifies the free ssDNA boundary. The extreme double or single strand ends are not protected in these assays even at high concentrations of *Sso*Dpo1 (2 μM).

Stoichiometric fluorescence anisotropy of *Sso*Dpo1 binding to DNA

To learn more about the stoichiometry of *Sso*Dpo1–DNA complex, we monitored the increase in fluorescence anisotropy upon *Sso*Dpo1 binding to fluorophore-labeled DNA (Figure 3A). Fluorescence anisotropy monitors the relative rotational diffusion rates of molecules so that an increase in molecular mass upon complex formation produces an increase in anisotropy. A ptDNA hairpin labeled with fluorescent dye, Cy5, at the 5′-end was used as a substrate (see the 'Materials and Methods' section). This hairpin eliminates a potential binding site at the double strand end known to be a binding site for some polymerases (34). The concentration of this fluorescent DNA substrate used in these experiments (400 nM) is higher than normally used to measure dissociation constants (K_d) so that stoichiometry can be monitored.

Binding of *Sso*Dpo1 to DNA was monitored by the increase in anisotropy upon addition of protein. The titration curve is also characterized by a steep slope for *Sso*Dpo1:DNA ratio < 1, a more shallow slope for 1 < *Sso*Dpo1:DNA ratio < 3 followed by saturation at *Sso*Dpo1:DNA ratio > 3. Such stoichiometric titration curve behavior indicates the presence of at least two different types of *Sso*Dpo1–DNA complexes. The approximate slopes of the individual binding events are shown along with their apparent stoichiometries (Figure 3A). Note that changing the initial DNA concentration 2-fold does not change stoichiometry (data not shown). Based on the magnitude of anisotropy change associated with each slope before a breakpoint, we suggest that the initial complex monitors formation of a 1:1 *Sso*Dpo1:DNA ratio and the other with a 3:1 ratio (Figure 3A). There are not sufficient data to detect an additional slope associated with a 2:1 *Sso*Dpo1:DNA ratio. However, we were able to determine an absolute stoichiometry of *Sso*Dpo1 to DNA of 3:1 and show that formation of this complex proceeds through a higher affinity 1:1 state.

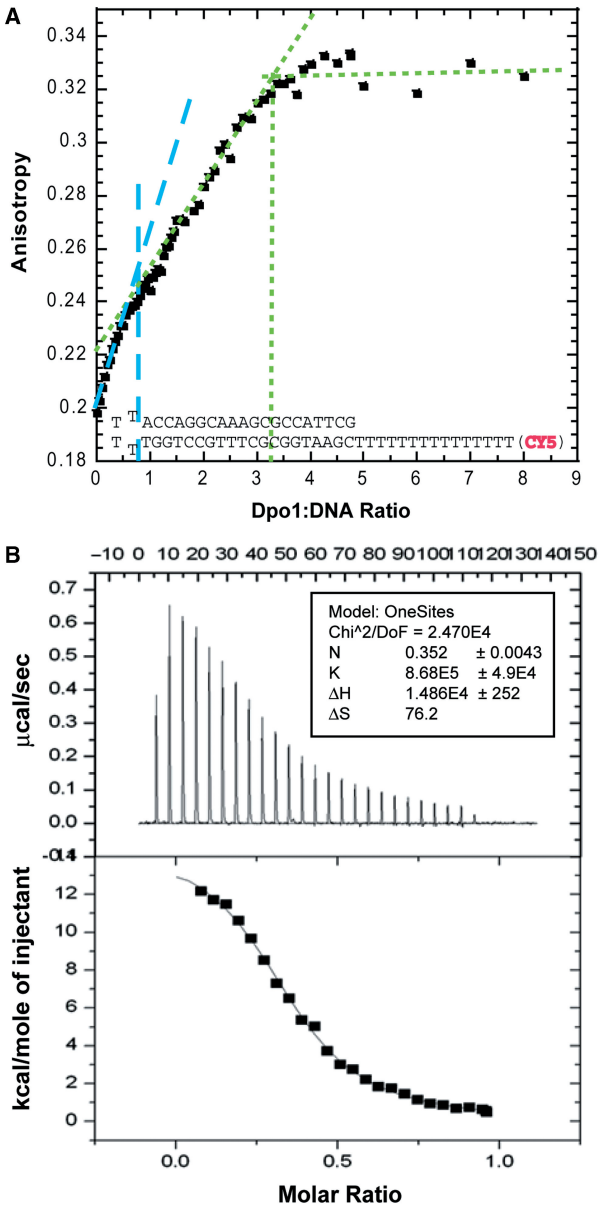

Figure 3. Quantifying stoichiometry of *Sso*Dpo1 binding to DNA. (**A**) Dependence of fluorescence anisotropy of labeled DNA hairpin (see the 'Materials and Methods' section) on *Sso*Dpo1:DNA stoichiometry. DNA concentration was fixed at 400 nM while the concentration of *Sso*Dpo1 was increased to give the stoichiometry listed on the *x*-axis. Cy5 was excited at 645 nm and an increase in anisotropy corresponding to a decrease in rotational diffusion due to *Sso*Dpo1 binding was monitored at 675 nm. Fits to the approximate limiting individual slopes are used to extrapolate the stoichiometry of the two binding phases for a monomeric-bound *Sso*Dpo1 (blue dash) and trimeric *Sso*Dpo1 complex (green dot). (**B**) ITC titration of primer/template (21/31-mer) DNA substrate into *Sso*Dpo1. Data was fit using Origin software and Equation (6) to yield thermodynamic parameter (ΔH°) 14.86 ± 0.252 kcal mol^{-1}, equilibrium association constant (K_a) $8.68 \times 10^5 \pm 4.9 \times 10^4$ M and stoichiometry (n) 0.352 ± 0.043 DNA: *Sso*Dpo1.

ITC to determine thermodynamic parameters of *Sso*Dpo1 binding

ITC was used to determine the stoichiometry and thermodynamic parameters for *Sso*Dpo1 binding to the short primer/template (21/31-mer) substrate (Figure 3B).

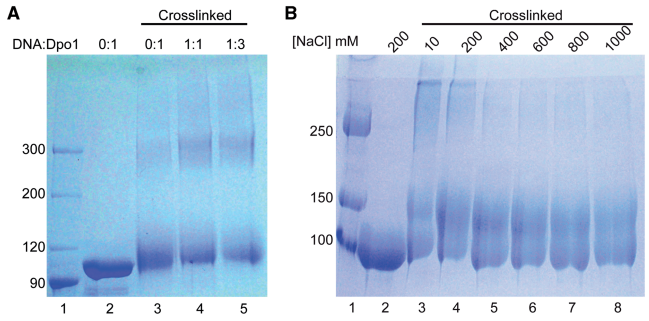

Figure 4. Covalent protein crosslinking of *Sso*Dpo1. (**A**) Performed in the absence and presence of different ratios of primer-template DNA. Lane 1: protein ladder, lane 2: *Sso*Dpo1 without modification, lane 3: *Sso*Dpo1 plus crosslinker, lane 4: *Sso*Dpo1–DNA complex plus crosslinker (1:1 *Sso*Dpo1:DNA ratio), lane 5: *Sso*Dpo1–DNA complex plus crosslinker (3:1 *Sso*Dpo1:DNA ratio). (**B**) Covalent protein crosslinking of 10 μM *Sso*Dpo1 performed at different concentrations of NaCl (10–1000 mM) in the presence of 100 nM ptDNA (21/31). Lane 1: protein ladder, lane 2: *Sso*Dpo1:DNA without modification, lanes 3–8: *Sso*Dpo1:DNA plus crosslinker at different [NaCl].

From a fit to the binding isotherm generated from titration of p/tDNA into a cell containing *Sso*Dpo1, the following parameters were calculated for the reaction at 30°C according to Equation 6: an apparent equilibrium association constant (K_A) of 8.7 ($\pm$0.5) $\times 10^5\,M^{-1}$ (i.e. $K_D = 1.2 \pm 0.1\,\mu M$), an endothermic ΔH° of $14.9\,kcal\,mol^{-1}$ and a stoichiometry of 2.84 ± 0.04 *Sso*Dpo1:DNA. Based on these values, the binding free energy ($\Delta G^\circ = -RT\ \ln\ K_A$) is $-8.2\,kcal\,mol^{-1}$ and $T\Delta S^\circ$ is $23.1\,kcal\,mol^{-1}$. Thus at 30°C, the binding of *Sso*Dpo1 to the 21/31 primer/template is enthalpically unfavorable and entropically favorable. However, if there is a large negative heat capacity change (i.e. strong temperature dependences for ΔH° and ΔS°) for *Sso*Dpo1 polymerase binding to DNA, we anticipate that at the physiological temperature (~75°C) for *S. solfataricus*, the driving force for the formation of the *Sso*Dpo1–DNA complex will switch from entropy to enthalpy. This has been shown for Taq and Klentaq DNA polymerases (35). For Taq and Klentaq polymerase, the minimum for ΔG° is near 50°C, but for *Sso*Dpo1 the minimum may occur at even higher temperatures. Reverse titrations of *Sso*Dpo1 into DNA would give information (similar to the EMSA results) about the individual K_ds of binding single and multiple polymerases or ΔC^o_P for the monomeric *Sso*Dpo1 form, but could not be performed due to *Sso*Dpo1 precipitation at the high concentration required. Nevertheless, the stoichiometry for the overall binding reaction can be measured in these experiments and is consistent with both the EMSA and anisotropy experiments showing a trimer of *Sso*Dpo1 capable of binding to primer/template DNA.

Protein chemical crosslinking of a *Sso*Dpo1 complex

To directly show the physical contact between *Sso*Dpo1 molecules alone and in complex with DNA, we employed chemical crosslinking. Covalent crosslinking of multimeric forms of proteins can be easily detected by SDS–PAGE (36). We used a Sulfo-EGS crosslinker containing two amine-reactive groups—NHS esters, connected with a relatively short linker (16.1 Å length), so that only protein amino groups in close proximity can be covalently modified.

Crosslinking of free *Sso*Dpo1 and in presence of DNA at two *Sso*Dpo1:DNA ratios (1:1 and 3:1) produced two distinct complexes (Figure 4A). Whereas only one band at 101 kDa is seen for unmodified *Sso*Dpo1, addition of crosslinker leads to the appearance of the second band at roughly ~303 kDa. Trimeric *Sso*Dpo1 can be captured over a range of NaCl concentrations up to 600 mM (Figure 4B). The molecular weight band is consistent with a trimer of *Sso*Dpo1. Surprisingly, this trimer band is also present in the absence of DNA. Because no complex of *Sso*Dpo1 in the absence of DNA was found by analytical gel filtration, we suggest that the interaction is transient at the concentrations of *Sso*Dpo1 used in the gel filtration analysis and only detectable by covalent capture of this complex. Addition of DNA significantly increases the amount of crosslinked trimer complex suggesting the presence of a more stable complex consistent with the gel filtration experiments. At the same time, there is no significant difference when crosslinking is performed at two different concentrations of *Sso*Dpo1, over a range of different temperatures, or using different DNA substrates (Figure 4 and data not shown). It should be noted that no *Sso*Dpo1 dimer—either with or without DNA—is observed possibly due to the lower relative abundance of a dimeric species as well as the detection limits of coomassie staining. It is probable, that in the time and concentrations used to perform the crosslinking experiments, very little dimer is present due to the cooperative association and capture this complex into the trimeric state, effectively reducing the dissociation to zero. Alternatively, simultaneous binding of two *Sso*Dpo1 molecules to different sites on *Sso*Dpo1 may be favored in this case.

Polymerization kinetics at different oligomeric states of *Sso*Dpo1

We tested the polymerization kinetics of both monomeric and trimeric *Sso*Dpo1–DNA complexes at 60°C. Traditional polymerase extension assays using a primed M13 substrate were performed at different concentrations of *Sso*Dpo1, quenched after 2 min, and then separated on an alkaline agarose gel (Figure 5A). Quantification of the average rate of synthesis based on the size of the DNA was performed by comparing to Λ/HindIII DNA standards in *lane* 1 using the ImageQuant software. The measured polymerization rate was vastly different at concentrations shown to be primarily monomer (<200 nM) versus those that are primarily trimer (>750 nM). A fit of the polymerization data to Equation 7 was more consistent with a cooperativity model for kinetic activity (Figure 5B) to give a kinetic K_d for *Sso*Dpo1 of 542 ± 5 nM and a maximal rate (V_{max}) of $422 \pm 4\,bp\,min^{-1}$. A positive cooperativity constant associated with this fit was 14 ± 1. Thus, the formation of a trimeric *Sso*Dpo1 is required for maximal activity of

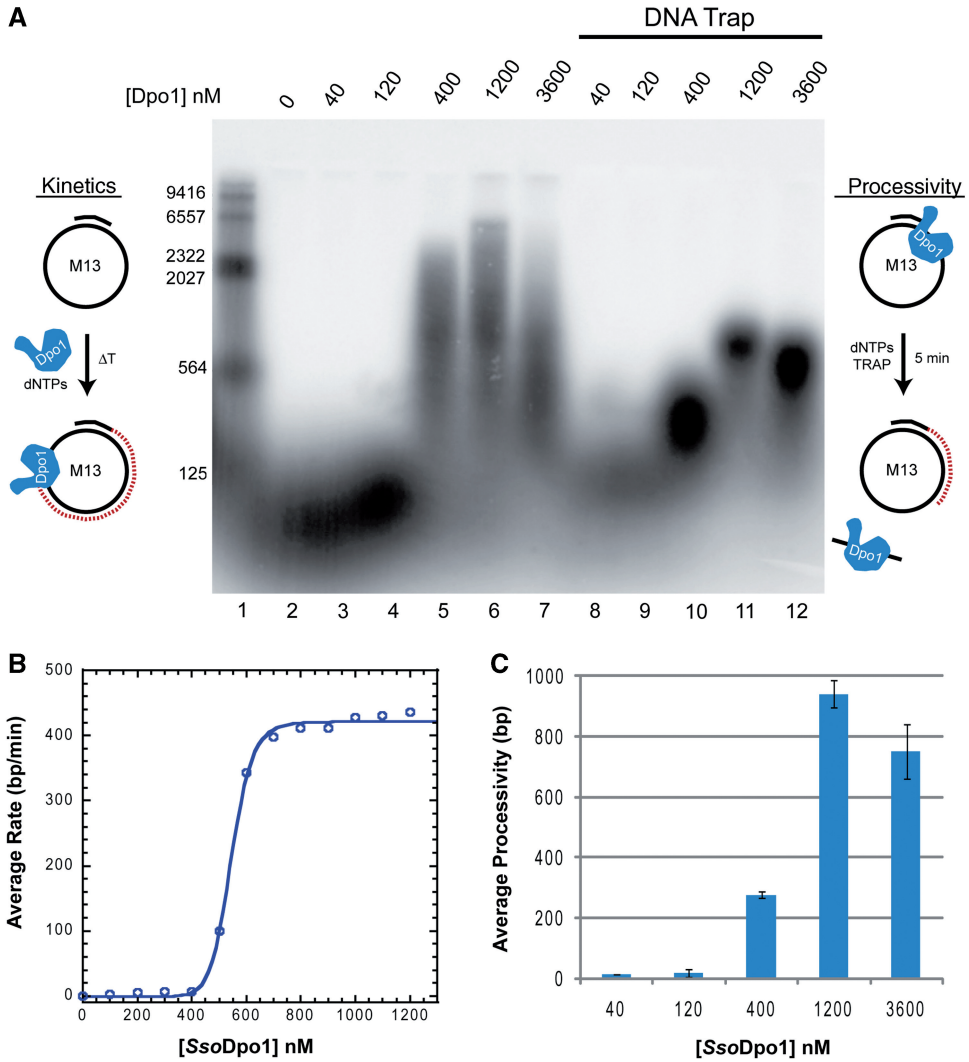

Figure 5. (**A**) Polymerase experiments were performed on primed M13 in the absence or presence of a DNA trap to monitor processivity at different concentrations of *Sso*Dpo1. A 5000-fold excess of ssDNA trap was added with dNTPs to initiate the reaction and then bind any dissociated *Sso*Dpo1 to prevent further synthesis. Experiments were quenched after 5 min and analyzed on an alkaline agarose gel for products >100 bases. Lanes 2–7 are kinetic experiments used to show the rate of DNA synthesis as a function of [*Sso*Dpo1]. Lanes 8–12 are identical to lanes 2–7 except that ssDNA trap was included to monitor processivity as a function of [*Sso*Dpo1] concentration. (**B**) Experiments covering a more complete range of *Sso*Dpo1 concentrations were performed and quenched at an identical 2-min time point. The rate of polymerization is calculated as the length of DNA synthesized divided by the time (bp/min) as calculate from the standard molecular weight markers (M) using ImageQuant software. Data was fit using Equation (7) for positive allostery to yield the following parameters: K_d = 543 ± 5 nM and V_{max} = 422 ± 4 bp min^{-1}. (**C**) The average length of DNA synthesized as a function of [*Sso*Dpo1] when DNA trap is included (lanes 8–12 in A) was calculated from the molecular weight markers using ImageQuant software.

this enzyme. This catalytic K_d is slightly higher than the binding constant for the trimeric complex determined in our EMSAs (Table 1). This suggests that fully formed trimeric *Sso*Dpo1 that approaches binding saturation in Figure 2E is necessary for optimal kinetic activity. At higher concentrations of enzyme (>2 μM), we consistently see a decrease in the kinetic rate. We suspect this is enzyme inhibition due to binding and blocking of additional sites on the single strand region of M13. This would cause an impediment to the active polymerase complex, and although the polymerase roadblock can be removed by the active one, it requires a certain amount of time that negatively affects the overall rate of synthesis.

We also performed identical kinetic assays on short ptDNA (21/31) to eliminate the possibility of binding multiple molecules laterally along the length of the DNA substrate. Due to the rate of synthesis measured above, these experiments were performed at 37°C and quenched after 10 s and shown and quantified in Supplementary Figure S3A and B. Similar kinetic constants and coopertivity curves to those fit above were also determined for the short ptDNA template confirming an active trimeric form of *Sso*Dpo1.

As can be seen from Figure 5, concentrations of *Sso*Dpo1 that are primarily monomer have a rate of synthesis of <50 bases min^{-1}, while the trimer rate is >300 bases min^{-1}. Because we can detect the rate of synthesis

from the average length of DNA products independent of the total amount of fully extended product, we are specifically examining how the oligomeric state of *Sso*Dpo1 influences the rate of synthesis and not the quantity of product formation. Under these conditions, the rate of synthesis is influenced by the off-rate and subsequent on-rate of either the monomeric or trimeric forms of *Sso*Dpo1. In these experiments, increasing the concentration of enzyme will naturally increase the re-association rate dependent on the K_d to produce longer DNA products. In order to examine the effect of monomer or trimer on the rate of DNA synthesis independent of re-association events, we utilized single-turnover experiments.

Polymerase processivity at different oligomeric states of *Sso*Dpo1

In these single-turnover assays, the length of DNA synthesized prior to dissociation from the DNA template is measured. Once *Sso*Dpo1 dissociates from the primed M13 template, it is trapped by binding to a high concentration of cold primer/template DNA substrate. We titrated the concentration of ssDNA trap needed to obtain a consistent processivity value and found that a 5000-fold excess of primer-template DNA was sufficient to trap all dissociated *Sso*Dpo1 as to not rebind the ^{32}P-labeled substrate and further influence our results (data not shown).

Due to the range in processivity lengths that we found dependent on the concentration of *Sso*Dpo1, we separated the products on a denaturing acrylamide (short DNA fragments <100 bases) and alkaline agarose ((long DNA fragments >100 bases) gels (Figures S4 and 5A). For concentrations of *Sso*Dpo1 that are mostly monomeric (120 nM), we measured an average processivity value of 18 ± 6 bases. This is consistent with processivity values measured for other polymerases in the absence of accessory factors (37–39). Upon increasing the concentration of *Sso*Dpo1 to promote trimer formation, the maximal processivity value increased roughly 500-fold to 942 ± 46 bases (Figure 5C). Similar to the kinetic data above, higher concentrations of *Sso*Dpo1 (>2 μM) show a reduction in processivity. This can be attributed to binding of additional molecules of *Sso*Dpo1 along the single strand region of M13 that can prematurely displace an active trimeric *Sso*Dpo1 complex.

As above and to test single monomeric or trimeric *Sso*Dpo1 complexes on DNA, we utilized the short ptDNA substrate (21/31) in similar single-turnover experiments at 37°C and quenched after 10 s (Figure S3C and D). Once again, the data matched a cooperative fit similar to Figure 5C where the trimeric *Sso*Dpo1 is required for maximal processivity.

Due to greater processivity, the trimeric *Sso*Dpo1 complex is more stable on the DNA substrate such that the off-rate is greatly reduced. By taking the rates of DNA synthesis and the processivity values for the monomeric and trimeric *Sso*Dpo1 (Figure 5), we can calculate the off-rates as $2\,min^{-1}$ and $0.5\,min^{-1}$, respectively. A 4-fold decrease in the off-rate for the trimeric *Sso*Dpo1 over that of the monomeric form promotes both an increase in the DNA synthesis ability and processivity for the enzyme complex.

DISCUSSION

*Sso*Dpo1 is one of the four predicted DNA polymerases contained within the genome of *S. solfataricus* and has been proposed to be the main DNA replication polymerase (6). Despite this, there was no detailed information about the binding thermodynamics or kinetics of this polymerase to DNA. In most respects, *Sso*Dpo1 is structurally and enzymatically similar to other DNA polymerases from the B-family except for an insertion in the fingers domain of the enzyme proposed to play a role in stabilization between the exonuclease and polymerase domains as well as a potential *Sso*Dpo4 interaction site (13,17). This unique insertion in *Sso*Dpo1 may act as a landing pad for other proteins within the context of DNA replication or repair, or it may serve to form the trimeric *Sso*Dpo1 complex described here.

In this study, the binding of *Sso*Dpo1 to DNA was found to induce and stabilize the formation of a trimeric DNA polymerase complex that activates polymerization. Formation of the trimeric form of the polymerase has important implications in the enzymatic activities of this enzyme complex that occur during DNA replication. Higher-affinity binding to the 3′OH of the first polymerase followed by cooperative formation of the trimeric polymerase complex is consistent with the read-ahead function of this polymerase in detecting lesions on the template strand (40,41).

Monomeric, dimeric and trimeric polymerase complexes are detected on p/tDNA substrates

During protein purification and in the absence of DNA substrates, *Sso*Dpo1 exists stably and solely as a monomer as shown by the analytical gel filtration studies even at very high concentrations (>20 μM) after elution from the column. Primer/template DNA was shown to shift the molecular mass of the complex to multiple forms consistent with a monomeric, dimeric and trimeric form of *Sso*Dpo1 bound to DNA. Initial binding of *Sso*Dpo1 to primer/template DNA depends slightly on template length, as a monomeric *Sso*Dpo1–DNA complex was not reproducibly detected by EMSA with the 21/31-mer substrate but more easily observed with a longer primer/template strand. DNA polymerases are known to bind with higher affinity to the 3′OH of the primer strand in the active site to discriminate incorporation of the next nucleotide from the template strand, so it is not surprising that *Sso*Dpo1 binds to this junction. What is surprising is the observation that an additional two molecules of *Sso*Dpo1 bind cooperatively to the initial *Sso*Dpo1/DNA complex.

The cooperative formation of a trimeric complex occurs at a higher dissociation constant than the monomeric form, but it is not outside the dissociation constant (K_d) realm of polymerase DNA interactions

detected previously and is within a physiological concentration range to be biologically relevant for replication proteins held at the replication fork (17,42,43). In support, Zhang *et al.* (44) has shown what we suspect to be a monomeric EMSA of *Sso*Dpo1 (300 nM) interacting with Orc/Cdc6 homologs while also reporting alterations in *Sso*Dpo1 activity at trimeric concentrations (900 nM). This shows that both monomeric and trimeric forms of *Sso*Dpo1 can have specific interactions with other proteins that modulate its activity.

Specific protein–protein interactions within *Sso*Dpo1 are responsible for trimerization on a variety of DNA substrates

A stoichiometry of three molecules of *Sso*Dpo1 to one molecule of DNA was observed for binding to different DNA substrates in four independent assays including: analytical gel filtration, EMSA, fluorescent anisotropy and ITC experiments. Although trimeric polymerase complexes form with single stranded, double stranded and primer/template substrates, the trimer of *Sso*Dpo1 has the highest affinity for the primer/template substrate due to the presence of a 3′-OH at the primer/template junction. The relative global binding affinities of this trimeric polymerase complex for other DNA substrates varied little (Table 1), highlighting a possible nondiscriminating binding mode resulting from specific protein–protein interactions of the second and third polymerase with the first. The first molecule of *Sso*Dpo1 differentiates between DNA substrates (ss-, ds- versus p/t) due to the identification of a monomeric *Sso*Dpo1 shift in our EMSA experiments with p/tDNA at lower concentrations. Cooperative formation of the trimeric complex then occurs at higher concentrations. Both the detection and quantification of trimeric *Sso*Dpo1 on short p/tDNA (21/31) where only a single molecule of *Sso*Dpo1 can bind laterally to the DNA as well as the restricted binding to the primer-template junction even at high concentrations of *Sso*Dpo1 as detected by nuclease footprinting is consistent with preferential binding to the primer-template junction and subsequent *Sso*Dpo1 binding directly to the primary polymerase.

In support of this binding model, protein crosslinking identified the presence of a complex consisting of primarily a trimeric *Sso*Dpo1. Because our gel filtration results were never able to detect a complex larger than a monomer in the 'absence of DNA', we suspect that the K_d for the oligomerization in the absence of DNA is much higher, such that the off-rate is large. Protein crosslinking was able to capture this transient complex through the formation of a covalent bond between molecules. We were also never able to detect a polymerase complex larger than a trimer for shorter ptDNA substrates where only a single polymerase can be bound laterally on DNA. This is consistent with our gel filtration studies which also did not detect the presence of complexes >300 kDa.

Taken together, these findings allow us to propose a model for the trimeric complex of *Sso*Dpo1 bound to the primer-template substrate that encircles the DNA (Figure 6). In this model, one polymerase molecule is bound to DNA substrate in an active conformation while the two others have little or no contacts with DNA. In this model, one, two or all three *Sso*Dpo1 molecules can be accessible to binding cofactors such as PCNA. In fact, this proposed circular representation of the trimeric polymerase complex is reminiscent of the structure of the processivity factor, PCNA, known to increase processivity for monomeric *Sso*Dpo1 along with a variety of other DNA polymerases (15,45), and is most likely responsible for the increase in processivity that we detect with the trimeric complex. We have arranged our model in this fashion due to the absence of any species greater than a trimer as well as a means to explain the enhanced processivity of the trimeric species.

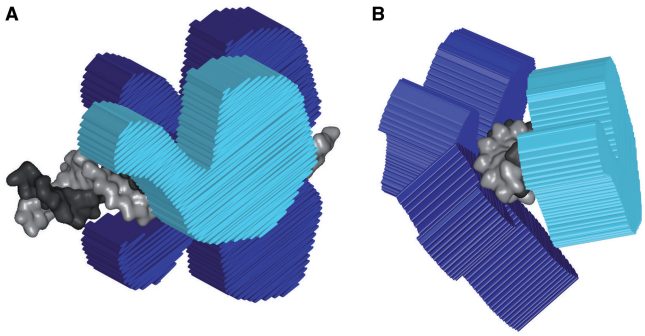

Figure 6. Hypothetical model of the *Sso*Dpo1 trimeric complex bound to the primer-template DNA substrate. (**A**) is rotated 90° to the right to obtain (**B**). The trimeric polymerase complex is shown to encircle the DNA substrate (gray). The active polymerase is in light blue, while the other two molecules are in darker blue and are not directly bound to the DNA template.

The monomeric and trimeric *Sso*Dpo1 complexes contribute differently to the kinetic proficiency of the polymerase

This is not the first example of a higher-order DNA polymerase complex, but it is the first trimeric-specific DNA polymerase complex of which we are aware. In *E. coli*, when three subunits of tau are incorporated into the gamma complex (clamp loader), a replisome can be constructed with three polymerases (23), but these are not specific polymerase–polymerase interactions. Instead, each polymerase is held in the replisome by specific interactions with the tau subunit. We determined the effect of having a monomeric or trimeric *Sso*Dpo1 complex assembled on DNA with the associated kinetic activity of both polymerization and processivity. Both the kinetic rate constant for polymerization as well as the processivity are increased with the trimeric *Sso*Dpo1. In fact, the kinetic rate data with increasing concentration of *Sso*Dpo1 also showed a cooperativity term similar to the binding data. Maximal DNA synthesis is achieved by the formation and associated activity of a trimeric *Sso*Dpo1. Therefore, depending on the concentration of the polymerase at the replication fork and accessibility of binding in the context of the entire replisome, the DNA synthesis ability can be controlled. This concentration dependence on the kinetics of polymerization is unlike

that shown for other B-family DNA polymerases from T4 or *E. coli* (21,46,47).

Single-turnover experiments that monitor how long a polymerase stays associated with the DNA template before dissociating clearly show that the trimeric *Sso*Dpo1 complex has a much greater processivity than that of the monomeric form. Therefore, the trimeric polymerase represents a dynamic complex able to promote the formation of longer DNA products before dissociation. Based on our model for binding (Figure 6), the active sites of the three polymerases are in a close enough proximity to the DNA template that they could easily exchange binding to the DNA template. We hypothesize that this mode of polymerase binding and active site switching is responsible for the increased processivity that we have observed. Transient dissociation from a DNA substrate by an individual molecule of *Sso*Dpo1 would allow for proximal binding of one of the other two molecules in the complex. Data presented here provide a general mechanism to increase polymerase processivity in the absence of cofactors due solely by polymerase oligomerization.

We have shown previously, that the DNA polymerase from bacteriophage T4 utilizes dynamic processivity mechanism to recruit additional molecules of the polymerase from solution to the replication fork during coupled leading and laggings strand synthesis (21). *Sulfolobus* may utilize a similar form of dynamic polymerase processivity in the absence of PCNA. We propose that multiple polymerases at the replication fork could also allow for alternative binding to the DNA substrate in the polymerase or exonuclease active sites to more effectively process the DNA substrate. The polymerase used in these experiments is devoid of exonuclease activity to allow for thermodynamic-binding measurements, so, we were unable to examine the exonuclease activities for the monomeric or trimeric forms. This ability to switch between polymerase and exonuclease active sites is essential in maintaining the high proofreading ability of this class of enzymes (48). *E. coli* Klenow (29) and rat polymerase β (49), show stoichiometries of two and four, respectively, on their DNA substrates. In the case of Klenow, binding of a dimeric complex in the polymerization mode is favored and may play a role in coordinating high-fidelity DNA synthesis.

The existence of multiple polymerase oligomeric forms allows for the possibility of differential functions of these complexes. This may be influenced and/or modified by the presence or absence of accessory factors, such as *Sso*PCNA, known to interact with *Sso*Dpo1. A trimeric polymerase complex may also build up in response to specific states of DNA conformations or in response to roadblocks, such as lesions, to DNA replication. Because of the lack of nucleotides in all our binding assays, we are simulating a stalled DNA polymerase so that we can measure the thermodynamics of binding to different DNA substrates. Within the cell, both thermodynamics and kinetics of binding conformation will determine the activities and states of complexes (either monomer or trimer); for example, in response to a lack of nucleotides, RNA primer handoff from the primase, DNA damage on the template strand or physical blocks to *Sso*Dpo1.

Theoretically, only two *Sso*Dpo1 molecules are necessary for a switch to occur between polymerase and exonuclease active sites. In addition to increasing processivity, the third DNA polymerase found in our complex may have a role in coordinating DNA synthesis on the lagging strand. In *E. coli* PolIII, the tau subunit acts to coordinate synthesis on the leading and lagging strands (23); however, the protein component or motif required for coupled DNA synthesis in eukaryotes and archaea has yet to be determined. The identification of this trimeric polymerase complex in *S. solfataricus* may be the first evidence for a polymerase complex capable of highly processive replication in the absence of accessory factors. Additionally, upon formation of the lagging strand holoenzyme, it is possible that another trimeric polymerase complex may also be associated with each Okazaki fragment. In any case, efficient processing of DNA in response to nucleotide selection, dNTP concentration pressures, proofreading and replication blocks, requires a dynamic polymerase complex capable of efficiently handling each scenario. The trimeric polymerase complex found in *Sso* may be an effective model system to study the coordination of these events.

SUPPLEMENTARY DATA

Supplementary Data are available at NAR Online.

FUNDING

University of Pittsburgh Department of Chemistry (to M.A.T.) and National Institutes of Health MERIT grant (5R37GM029207 to L.J.-J.). Funding for open access charge: University of Pittsburgh Department of Chemistry (to M.A.T.) and National Institutes of Health MERIT grant (5R37GM029207 to L.J.-J.).

Conflict of interest statement. None declared.

REFERENCES

1. Steitz,T.A. (1999) DNA polymerases: structural diversity and common mechanisms. *J. Biol. Chem.*, **274**, 17395–17398.
2. Kunkel,T.A. (2004) DNA replication fidelity. *J. Biol. Chem.*, **279**, 16895–16898.
3. Prakash,S., Johnson,R.E. and Prakash,L. (2005) Eukaryotic translesion synthesis DNA polymerases: specificity of structure and function. *Annu. Rev. Biochem.*, **74**, 317–353.
4. Braithwaite,D.K. and Ito,J. (1993) Compilation, alignment, and phylogenetic relationships of DNA polymerases. *Nucleic Acids Res.*, **21**, 787–802.
5. Burgers,P.M., Koonin,E.V., Bruford,E., Blanco,L., Burtis,K.C., Christman,M.F., Copeland,W.C., Friedberg,E.C., Hanaoka,F., Hinkle,D.C. *et al.* (2001) Eukaryotic DNA polymerases: proposal for a revised nomenclature. *J. Biol. Chem.*, **276**, 43487–43490.
6. Rogozin,I.B., Makarova,K.S., Pavlov,Y.I. and Koonin,E.V. (2008) A highly conserved family of inactivated archaeal B family DNA polymerases. *Biol. Direct.*, **3**, 32.
7. Pisani,F.M., De,F.M., Manco,G. and Rossi,M. (1998) Domain organization and biochemical features of Sulfolobus solfataricus DNA polymerase. *Extremophiles.*, **2**, 171–177.

8. Pisani,F.M., De,F.M. and Rossi,M. (1998) Amino acid residues involved in determining the processivity of the 3′-5′ exonuclease activity in a family B DNA polymerase from the thermoacidophilic archaeon Sulfolobus solfataricus. *Biochemistry*, **37**, 15005–15012.
9. Pisani,F.M., De,M.C. and Rossi,M. (1992) A DNA polymerase from the archaeon Sulfolobus solfataricus shows sequence similarity to family B DNA polymerases. *Nucleic Acids Res.*, **20**, 2711–2716.
10. Rella,R., Raia,C.A., Pisani,F.M., D'Auria,S., Nucci,R., Gambacorta,A., De,R.M. and Rossi,M. (1990) Purification and properties of a thermophilic and thermostable DNA polymerase from the archaebacterium Sulfolobus solfataricus. *Ital. J. Biochem.*, **39**, 83–99.
11. Lou,H., Duan,Z., Sun,T. and Huang,L. (2004) Cleavage of double-stranded DNA by the intrinsic 3′-5′ exonuclease activity of DNA polymerase B1 from the hyperthermophilic archaeon Sulfolobus solfataricus at high temperature. *FEMS Microbiol. Lett.*, **231**, 111–117.
12. Lou,H., Duan,Z., Huo,X. and Huang,L. (2004) Modulation of hyperthermophilic DNA polymerase activity by archaeal chromatin proteins. *J. Biol. Chem.*, **279**, 127–132.
13. Savino,C., Federici,L., Johnson,K.A., Vallone,B., Nastopoulos,V., Rossi,M., Pisani,F.M. and Tsernoglou,D. (2004) Insights into DNA replication: the crystal structure of DNA polymerase B1 from the archaeon Sulfolobus solfataricus. *Structure*, **12**, 2001–2008.
14. Dionne,I., Brown,N.J., Woodgate,R. and Bell,S.D. (2008) On the mechanism of loading the PCNA sliding clamp by RFC. *Mol. Microbiol.*, **68**, 216–222.
15. Dionne,I., Nookala,R.K., Jackson,S.P., Doherty,A.J. and Bell,S.D. (2003) A heterotrimeric PCNA in the hyperthermophilic archaeon Sulfolobus solfataricus. *Mol. Cell*, **11**, 275–282.
16. von Hippel,P.H., Fairfield,F.R. and Dolejsi,M.K. (1994) On the processivity of polymerases. *Ann. NY Acad. Sci.*, **726**, 118–131.
17. De,F.M., Medagli,B., Esposito,L., De,F.M., Pucci,B., Rossi,M., Gruz,P., Nohmi,T. and Pisani,F.M. (2007) Biochemical evidence of a physical interaction between Sulfolobus solfataricus B-family and Y-family DNA polymerases. *Extremophiles*, **11**, 277–282.
18. Indiani,C., McInerney,P., Georgescu,R., Goodman,M.F. and O'Donnell,M. (2005) A sliding-clamp toolbelt binds high- and low-fidelity DNA polymerases simultaneously. *Mol. Cell*, **19**, 805–815.
19. Moldovan,G.L., Pfander,B. and Jentsch,S. (2007) PCNA, the maestro of the replication fork. *Cell*, **129**, 665–679.
20. Ishmael,F.T., Trakselis,M.A. and Benkovic,S.J. (2003) Protein-protein interactions in the bacteriophage T4 replisome. *The leading strand loloenzyme is physically linked to the lagging strand holoenzyme and primosome*. *J. Biol. Chem.*, **278**, 3145–3152.
21. Yang,J., Zhuang,Z., Roccasecca,R.M., Trakselis,M.A. and Benkovic,S.J. (2004) The dynamic processivity of the T4 DNA polymerase during replication. *Proc. Natl Acad. Sci. USA*, **101**, 8289–8294.
22. Kim,S., Dallmann,H.G., McHenry,C.S. and Marians,K.J. (1996) tau couples the leading- and lagging-strand polymerases at the Escherichia coli DNA replication fork. *J. Biol. Chem.*, **271**, 21406–21412.
23. McInerney,P., Johnson,A., Katz,F. and O'Donnell,M. (2007) Characterization of a triple DNA polymerase replisome. *Mol. Cell*, **27**, 527–538.
24. Nick McElhinny,S.A., Gordenin,D.A., Stith,C.M., Burgers,P.M. and Kunkel,T.A. (2008) Division of labor at the eukaryotic replication fork. *Mol. Cell*, **30**, 137–144.
25. Kunkel,T.A. and Burgers,P.M. (2008) Dividing the workload at a eukaryotic replication fork. *Trends Cell Biol.*, **18**, 521–527.
26. Li,Y., Kong,Y., Korolev,S. and Waksman,G. (1998) Crystal structures of the Klenow fragment of Thermus aquaticus DNA polymerase I complexed with deoxyribonucleoside triphosphates. *Protein Sci.*, **7**, 1116–1123.
27. Beese,L.S., Friedman,J.M. and Steitz,T.A. (1993) Crystal structures of the Klenow fragment of DNA polymerase I complexed with deoxynucleoside triphosphate and pyrophosphate. *Biochemistry*, **32**, 14095–14101.
28. Beese,L.S., Derbyshire,V. and Steitz,T.A. (1993) Structure of DNA polymerase I Klenow fragment bound to duplex DNA. *Science*, **260**, 352–355.
29. Bailey,M.F., Van der Schans,E.J. and Millar,D.P. (2007) Dimerization of the Klenow fragment of Escherichia coli DNA polymerase I is linked to its mode of DNA binding. *Biochemistry*, **46**, 8085–8099.
30. Trakselis,M.A., Alley,S.C., Abel-Santos,E. and Benkovic,S.J. (2001) Creating a dynamic picture of the sliding clamp during T4 DNA polymerase holoenzyme assembly by using fluorescence resonance energy transfer. *Proc. Natl Acad. Sci. USA*, **98**, 8368–8375.
31. Gill,S.C. and von Hippel,P.H. (1989) Calculation of protein extinction coefficients from amino acid sequence data. *Anal. Biochem.*, **182**, 319–326.
32. Shuttleworth,G., Fogg,M.J., Kurpiewski,M.R., Jen-Jacobson,L. and Connolly,B.A. (2004) Recognition of the pro-mutagenic base uracil by family B DNA polymerases from archaea. *J. Mol. Biol.*, **337**, 621–634.
33. Pierce,M.M., Raman,C.S. and Nall,B.T. (1999) Isothermal titration calorimetry of protein-protein interactions. *Methods*, **19**, 213–221.
34. Eom,S.H., Wang,J. and Steitz,T.A. (1996) Structure of Taq polymerase with DNA at the polymerase active site. *Nature*, **382**, 278–281.
35. Datta,K. and LiCata,V.J. (2003) Thermodynamics of the binding of Thermus aquaticus DNA polymerase to primed-template DNA. *Nucleic Acids Res.*, **31**, 5590–5597.
36. Trakselis,M.A., Alley,S.C. and Ishmael,F.T. (2005) Identification and mapping of protein-protein interactions by a combination of cross-linking, cleavage, and proteomics. *Bioconjug. Chem.*, **16**, 741–750.
37. Tabor,S., Huber,H.E. and Richardson,C.C. (1987) Escherichia coli thioredoxin confers processivity on the DNA polymerase activity of the gene 5 protein of bacteriophage T7. *J. Biol. Chem.*, **262**, 16212–16223.
38. Jarvis,T.C., Newport,J.W. and von Hippel,P.H. (1991) Stimulation of the processivity of the DNA polymerase of bacteriophage T4 by the polymerase accessory proteins. *The role of ATP hydrolysis*. *J. Biol. Chem.*, **266**, 1830–1840.
39. Merkens,L.S., Bryan,S.K. and Moses,R.E. (1995) Inactivation of the 5′-3′ exonuclease of Thermus aquaticus DNA polymerase. *Biochim. Biophys. Acta*, **1264**, 243–248.
40. Greagg,M.A., Fogg,M.J., Panayotou,G., Evans,S.J., Connolly,B.A. and Pearl,L.H. (1999) A read-ahead function in archaeal DNA polymerases detects promutagenic template-strand uracil. *Proc. Natl Acad. Sci. USA*, **96**, 9045–9050.
41. Gruz,P., Shimizu,M., Pisani,F.M., De,F.M., Kanke,Y. and Nohmi,T. (2003) Processing of DNA lesions by archaeal DNA polymerases from Sulfolobus solfataricus. *Nucleic Acids Res.*, **31**, 4024–4030.
42. Lone,S., Townson,S.A., Uljon,S.N., Johnson,R.E., Brahma,A., Nair,D.T., Prakash,S., Prakash,L. and Aggarwal,A.K. (2007) Human DNA polymerase kappa encircles DNA: implications for mismatch extension and lesion bypass. *Mol. Cell*, **25**, 601–614.
43. Naktinis,V., Turner,J. and O'Donnell,M. (1996) A molecular switch in a replication machine defined by an internal competition for protein rings. *Cell*, **84**, 137–145.
44. Zhang,L., Zhang,L., Liu,Y., Yang,S., Gao,C., Gong,H., Feng,Y. and He,Z.G. (2009) Archaeal eukaryote-like Orc1/Cdc6 initiators physically interact with DNA polymerase B1 and regulate its functions. *Proc. Natl Acad. Sci. USA*, **106**, 7792–7797.
45. Trakselis,M.A. and Benkovic,S.J. (2001) Intricacies in ATP-dependent clamp loading. *Variations across replication systems*. *Structure*, **9**, 999–1004.
46. Yang,J., Trakselis,M.A., Roccasecca,R.M. and Benkovic,S.J. (2003) The application of a minicircle substrate in the study of the coordinated T4 DNA replication. *J. Biol. Chem.*, **278**, 49828–49838.
47. LaDuca,R.J., Fay,P.J., Chuang,C., McHenry,C.S. and Bambara,R.A. (1983) Site-specific pausing of deoxyribonucleic acid synthesis catalyzed by four forms of Escherichia coli DNA polymerase III. *Biochemistry*, **22**, 5177–5188.
48. Donlin,M.J., Patel,S.S. and Johnson,K.A. (1991) Kinetic partitioning between the exonuclease and polymerase sites in DNA error correction. *Biochemistry*, **30**, 538–546.
49. Jezewska,M.J., Rajendran,S. and Bujalowski,W. (2001) Energetics and specificity of Rat DNA polymerase beta interactions with template-primer and gapped DNA substrates. *J. Biol. Chem.*, **276**, 16123–16136.